

Supporting Information for:

Supramolecular Chemistry of Monochiral Naphthalenediimides

Tom W. Anderson,^a G. Dan Pantoş^{a,b} and Jeremy K. M. Sanders^a

^aUniversity Chemical Laboratory, University of Cambridge, Lensfield Road, Cambridge, CB2 1EW

^bDepartment of Chemistry, University of Bath, Bath, BA2 7AY

E-mail: g.d.pantos@bath.ac.uk; jkms@cam.ac.uk

Monochiral NDI solution CD spectra-----	S2
NMR coupling constants of the α -protons of L-1 and L-6 under methanolic conditions-----	S3
Formation of the C ₇₀ receptor by L-7 and L-8 -----	S4
NDI L-7 as a sergeant-----	S6
NDI 4 as a soldier-----	S6
Protocol for Figure 11 -----	S7
Raw Circular Dichroism Data-----	S7

Monochiral NDI CD spectra in methanolic solution

The CD spectra for each monochiral NDI (**L-6**, **L-7** and **L-8**) in two different solutions are compared: in 100% TCE and in 5% methanol 95% TCE. The nanotube (and other NDI hydrogen-bonded assemblies) does not form in the methanolic solution.¹ The disparity between the CD spectra in the two solutions demonstrates that all the NDIs hydrogen-bond to form nanotubes in 100% TCE solution, even when (as in the case of **L-8**) the size of the peak is much smaller than that of dichiral **L-1**.

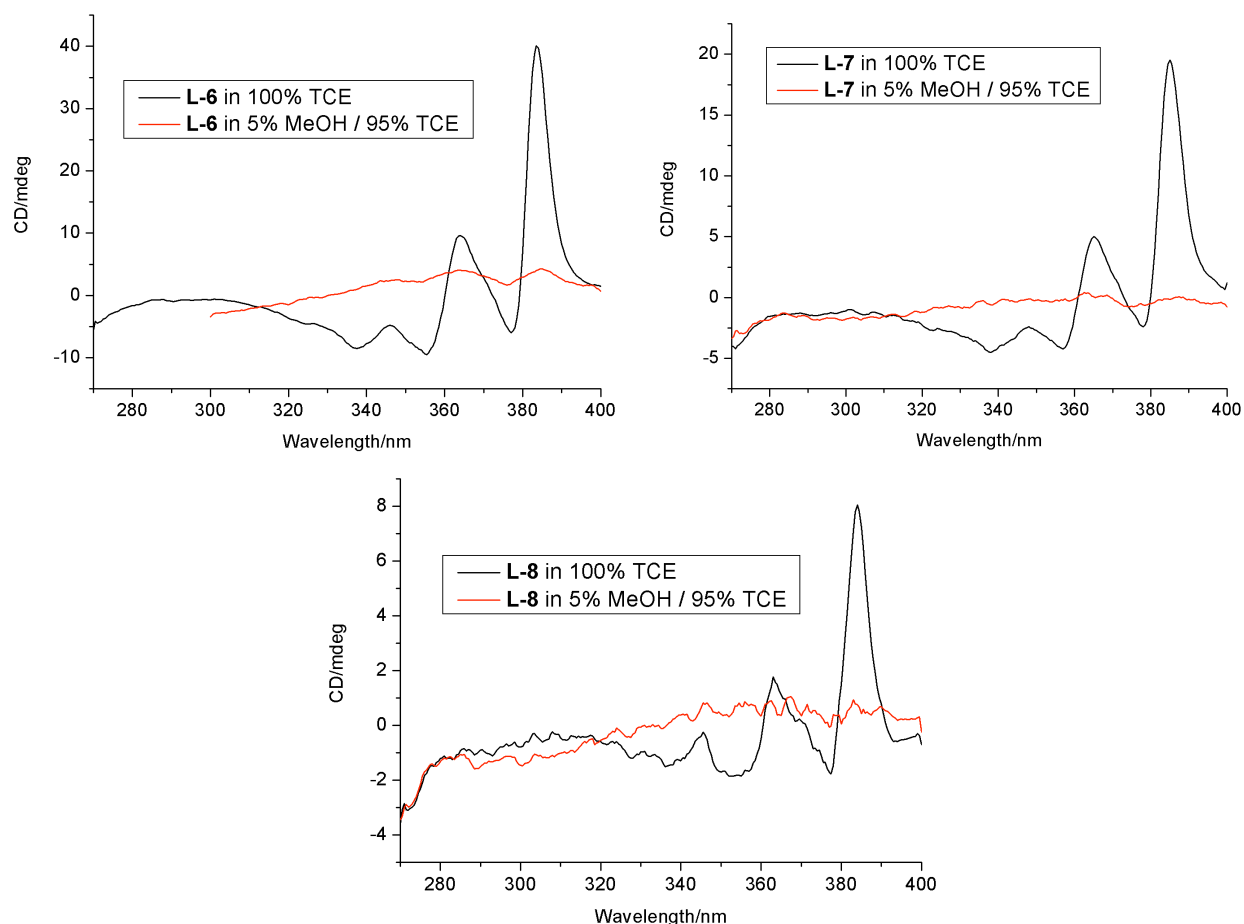


Figure S1. CD spectra for the three monochiral NDIs in 100% TCE and 5% MeOH / 95% TCE solutions. In each case the concentration of NDI in solution is $2.1 \times 10^{-4} \text{ mol dm}^{-3}$.

NMR coupling constants of the α -protons of L-1 and L-6 under methanolic conditions

The α -protons of dichiral **L-1** and monochiral **L-6** have characteristic different coupling constants when observed in deuterated TCE, suggesting a different geometry in the nanotube (**Figure 6** in the paper). **Figure S2** shows a control experiment in which the α -proton NMR of **L-1** and **L-6** are compared when the two are in methanolic solutions in which the nanotube cannot form. The coupling constants are now identical, confirming that the effect is—as expected—not observed in the NDI monomer, only in the nanotube.

L-6 in 5% MeOD / 95% deuterated TCE
L-1 in 5% MeOD / 95% deuterated TCE

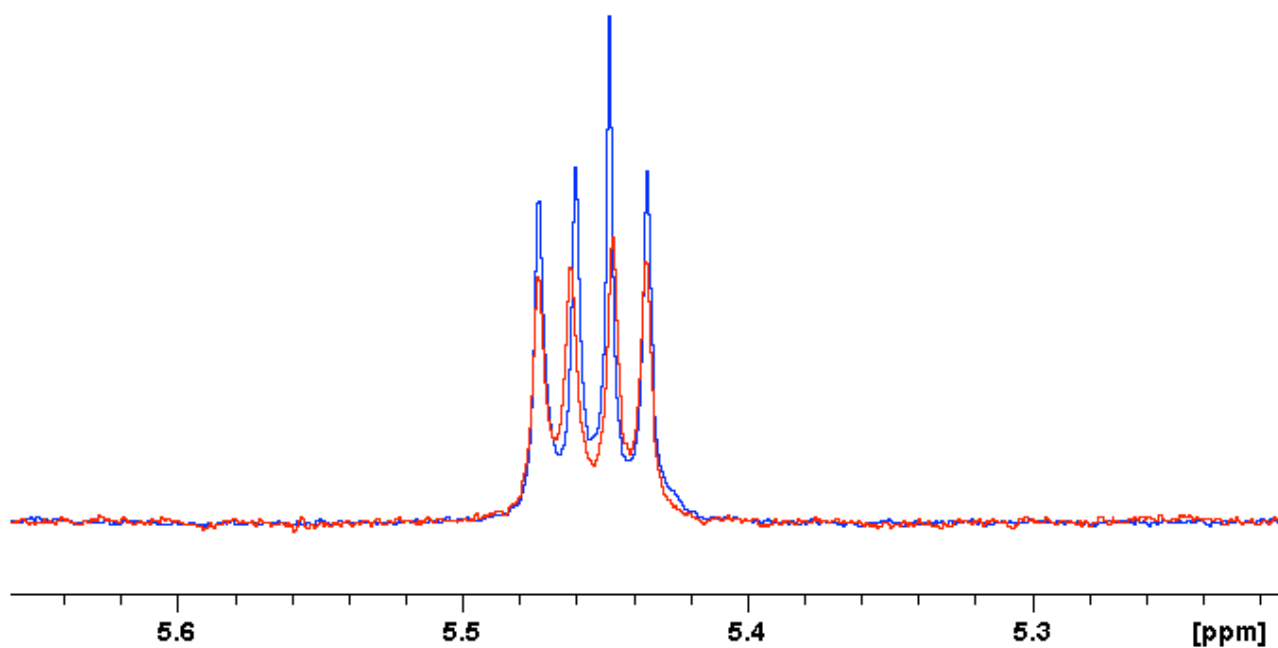


Figure S2. ^1H NMR of the α -protons of NDIs **L-1** and **L-6** in 5% MeOD / 95% TCE solution. Note that as **L-1** has two α -protons and **L-6** only one, the NMR traces are not on the same vertical scale.

Formation of the C₇₀ receptor by L-7 and L-8

As a companion to **Figure 8**, **Figure S3** shows the changes in the same parts of the ¹H NMR spectra of NDIs L-7 and L-8 when an excess of C₇₀ is added.

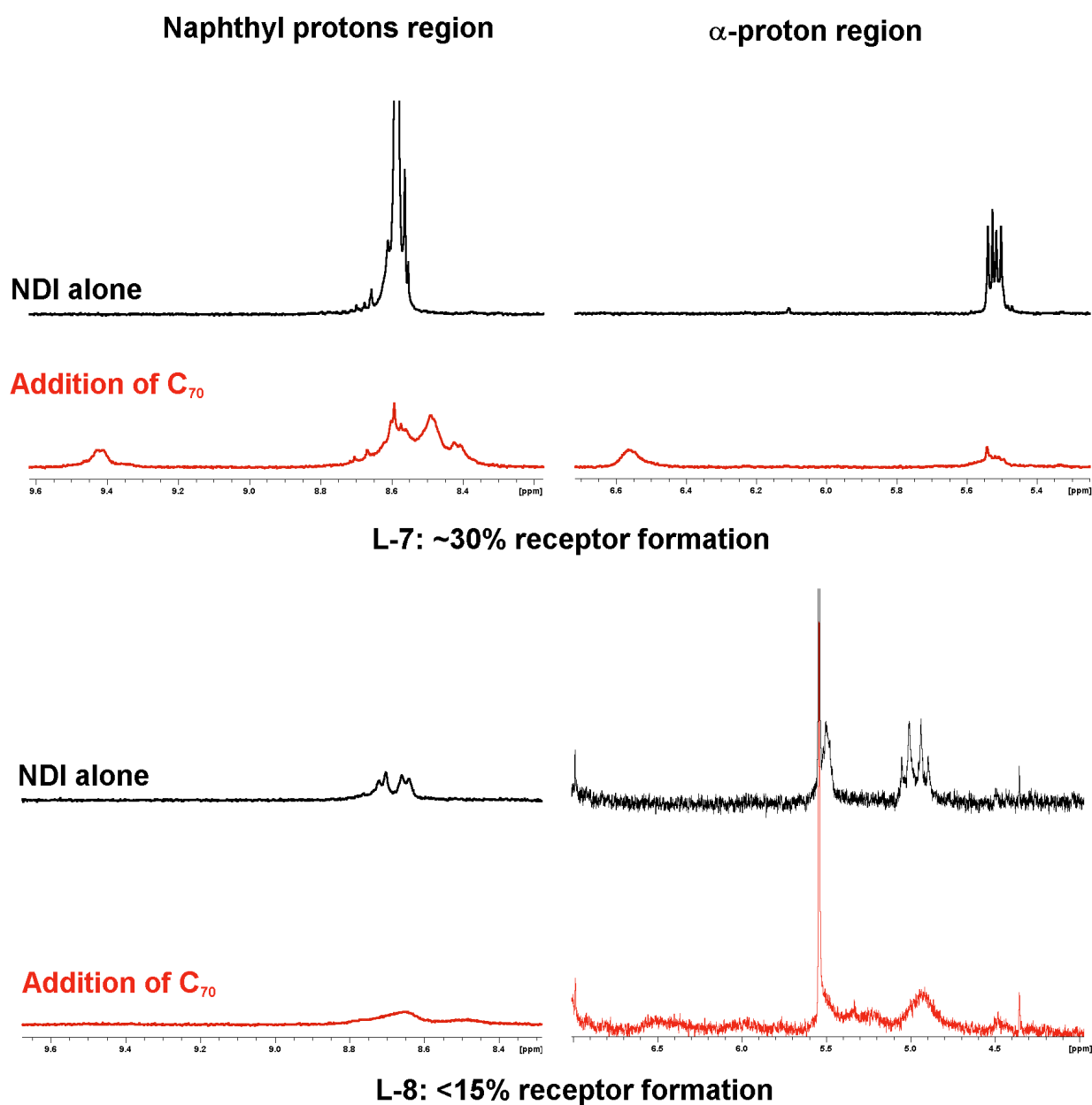


Figure S3. Changes in the ¹H NMR spectra of L-7 and L-8 on the addition of C₇₀. The solvent is CDCl₃.

In the case of L-8, solubility in CDCl₃ is low enough that the spectrum is subject to significant noise levels. **Figure S4** represents a magnification of the naphthyl protons section of the spectrum. The emergence of the characteristic four peaks associated with the C₇₀ receptor can just be observed, as one of the peaks is significantly downfield from the others. Only a small proportion of L-8 forms the receptor, but it does form.

NDI alone

Addition of C₇₀

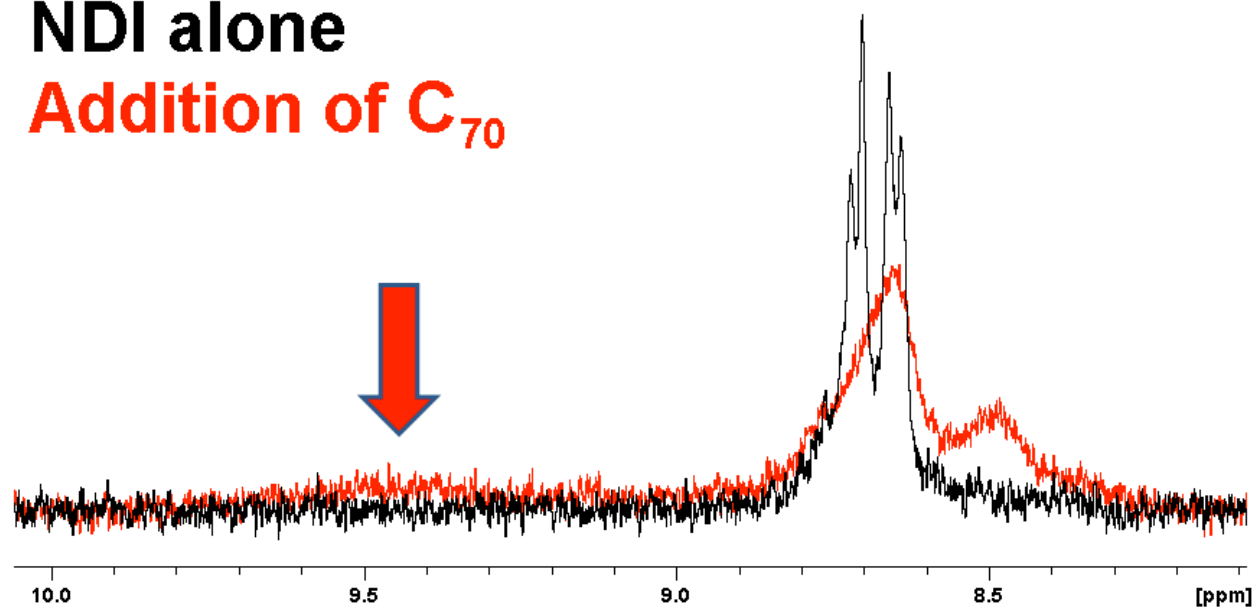


Figure S4. Magnification of the naphthyl protons section of the ¹H NMR spectrum for **L-8**, showing the change on the addition of C₇₀. The (broad) emerging peak is indicated with an arrow. The solvent is CDCl₃.

NDI L-7 as a sergeant

NDI L-7 has similar properties as a sergeant to L-6. **Figure S5** shows data from experiments using the same protocol as described in **Figure 10**, except that L-7 is substituted for L-6 as the sergeant used.

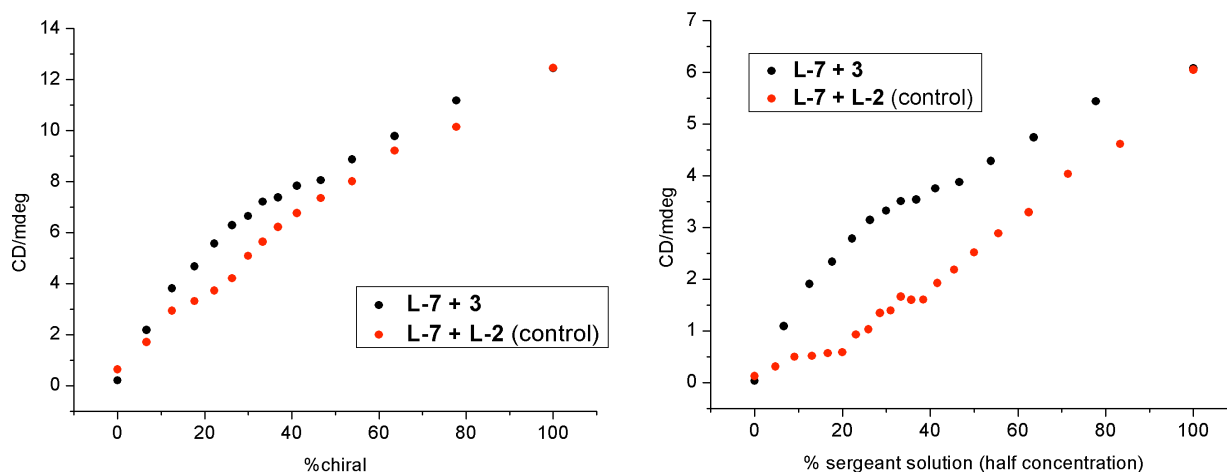


Figure S5. Sergeants-and-soldiers data with L-7 as the sergeant and 3 as the soldier. The left-hand graph shows data collected when the sergeant and soldier solutions are of the same concentration ($2.1 \times 10^{-4} \text{ mol dm}^{-3}$), while the right-hand graph shows data when the soldier solution is twice as concentrated ($2.1 \times 10^{-4} \text{ mol dm}^{-3}$) as that of the sergeant ($1.05 \times 10^{-4} \text{ mol dm}^{-3}$). See **Figure 10** and the main text for more details.

NDI 4 as a soldier

As reported previously with L-1 as a sergeant,² NDI 4 acts as a soldier with the monochiral NDIs as sergeants, but an inferior one to NDI 3. Example data is shown for L-7 as the sergeant for comparison to **Figure S5**.

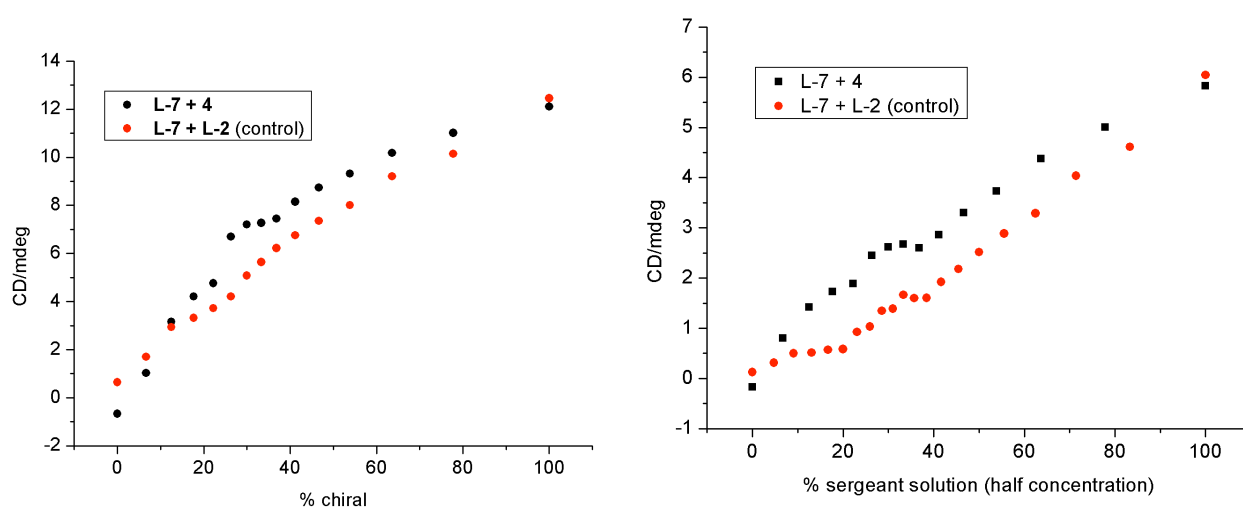


Figure S6. Sergeants-and-soldiers data with L-7 as the sergeant and 4 as the soldier. The left-hand graph shows data collected when the sergeant and soldier solutions are of the same concentration ($2.1 \times 10^{-4} \text{ mol dm}^{-3}$), while the right-hand graph shows data when the soldier solution is twice as concentrated ($2.1 \times 10^{-4} \text{ mol dm}^{-3}$) as that of the sergeant ($1.05 \times 10^{-4} \text{ mol dm}^{-3}$).

Protocol for **Figure 11**

Due to the weaker CD signal associated with NDI **L-8**, the standard experimental protocol runs had to be modified. The CD produced by the intrinsic chirality of ester **L-2** is no longer small enough that it may be ignored, distorting the the control experiment. Also, noise levels are such that the experimental datapoints for a single run show considerable error (**Figure S7**).

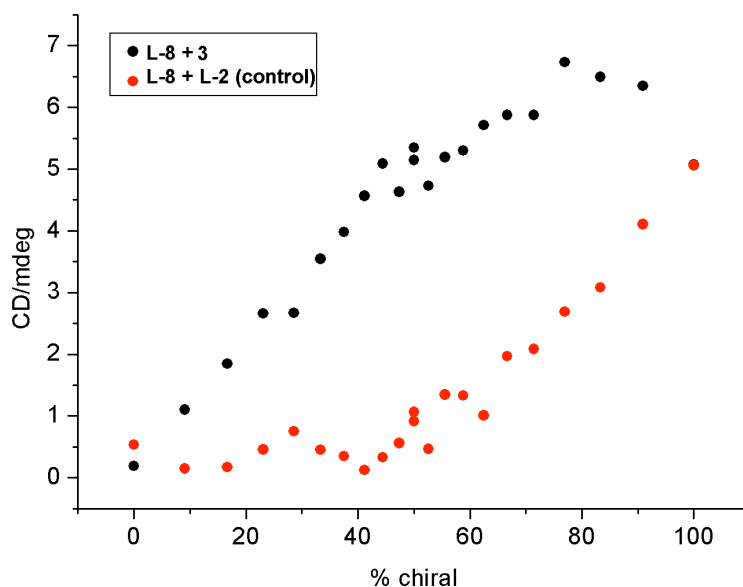


Figure S7. Attempting to use the standard experimental protocol with **L-8** leads to noisy data and a distorted control experiment. Concentration of both **L-2** and **L-8** solutions in TCE = 2.1×10^{-4} mol dm⁻³.

In order to produce the cleaner, usable data seen in **Figure 11**, two modifications were made to the protocol. Firstly the experiment was repeated three times and the traces averaged, considerably reducing error and smoothing the shape of the curve. Secondly, the usual control experiment was modified. Rather than adding a solution of ester **L-2** equal in concentration to the solution of **3**, an equal volume of pure TCE solvent was added. This type of control experiment is usually not ideal because it does not maintain a constant concentration of all NDIs in solution across the whole experiment. However, experiments with other NDIs that produce larger CD traces suggested that this change actually makes little difference to the control curve, meaning it was tolerated for this experiment when there was no alternative.

Raw Circular Dichroism Data

Raw data plots for the various CD plots shown in the paper are given below. All CD traces for a given experiment are shown with CD plotted against wavelength. The data is shown as recorded, before any corrections were applied. The scan region is either 270-400 or 300-400 nm, constrained at the lower end by the fact that tetrachloroethane absorbs around 250 nm.

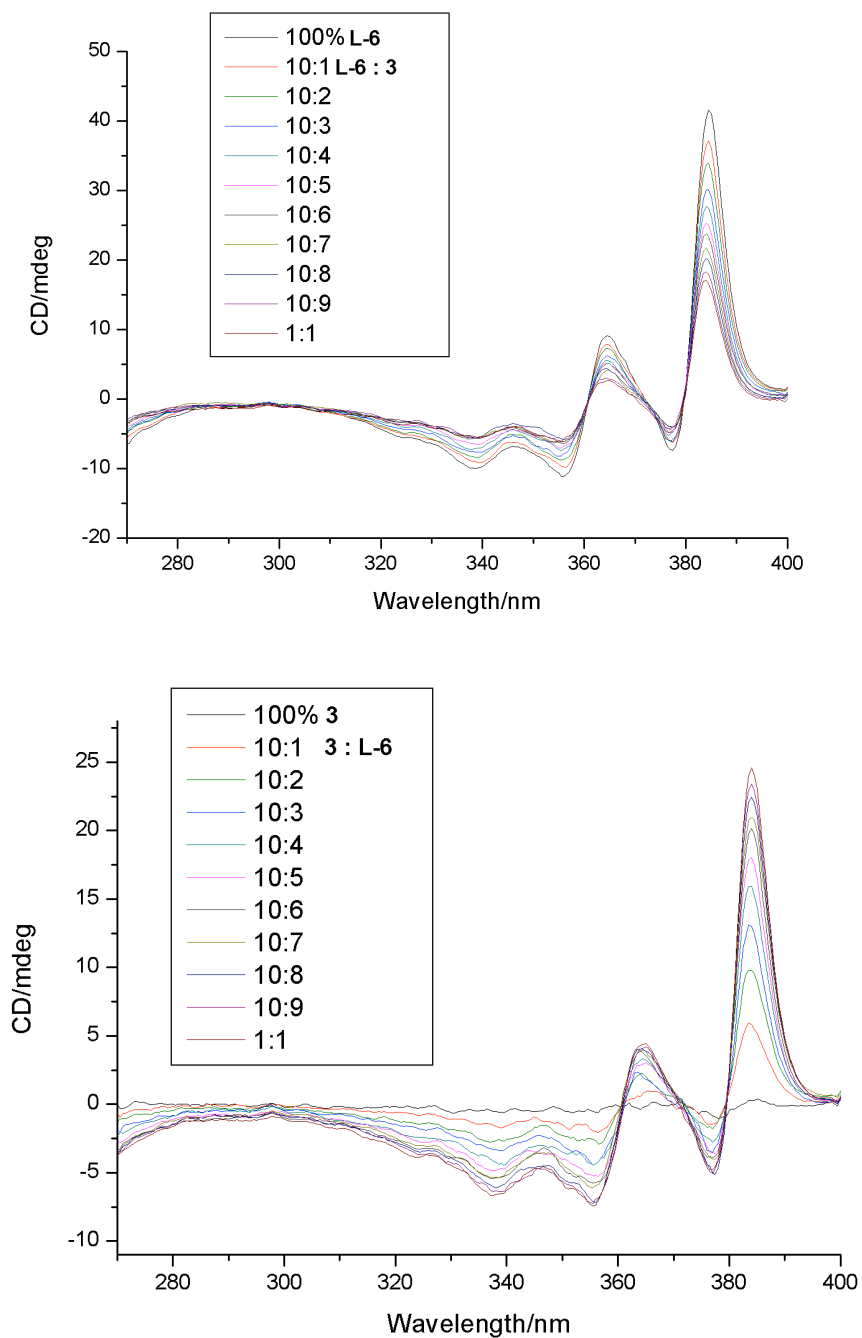


Figure S8. Raw experimental CD data for the first graph of **Figure 10** (black points). Concentration of both **3** and **L-6** solutions in TCE = 2.1×10^{-4} mol dm⁻³.

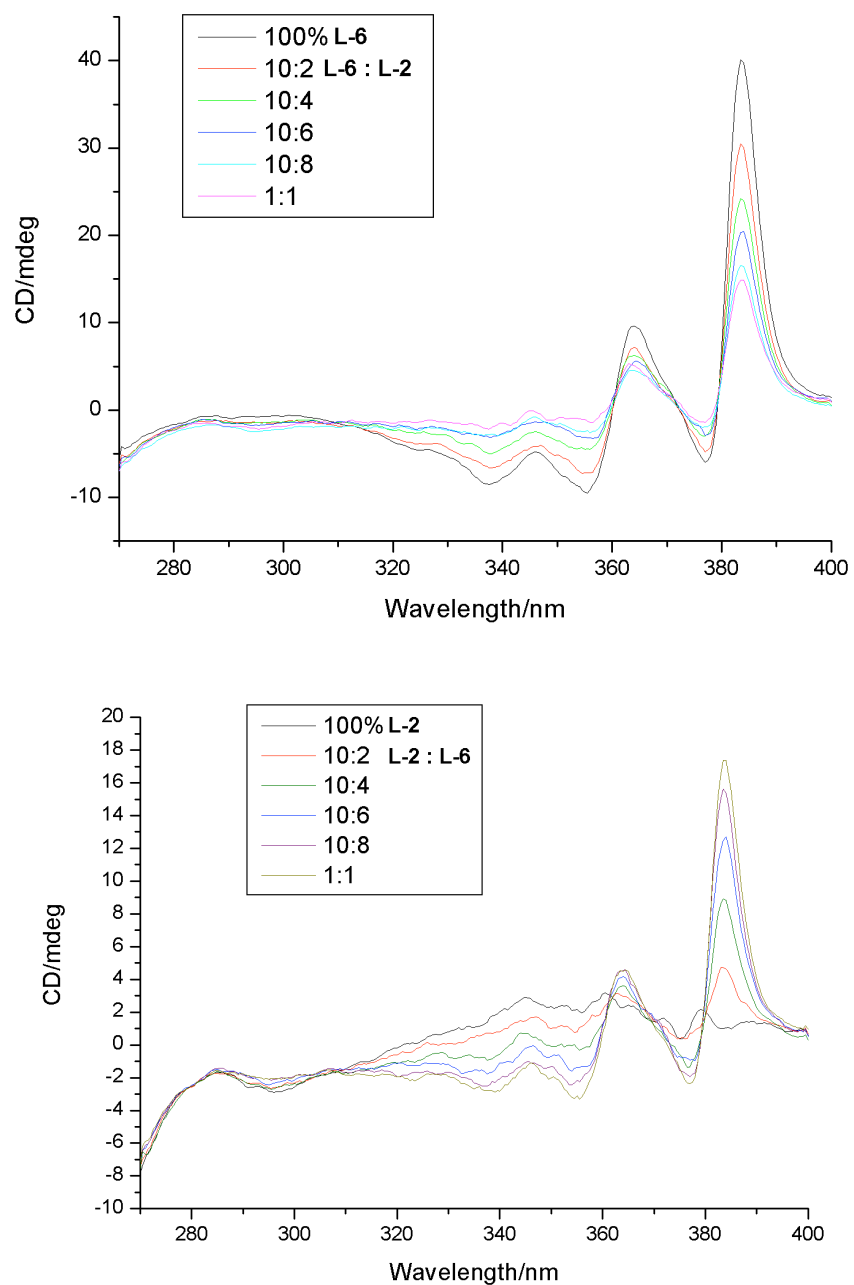


Figure S8. Raw control CD data for the first graph of **Figure 10** (red points). Concentration of both L-2 and L-6 solutions in TCE = 2.1×10^{-4} mol dm⁻³.

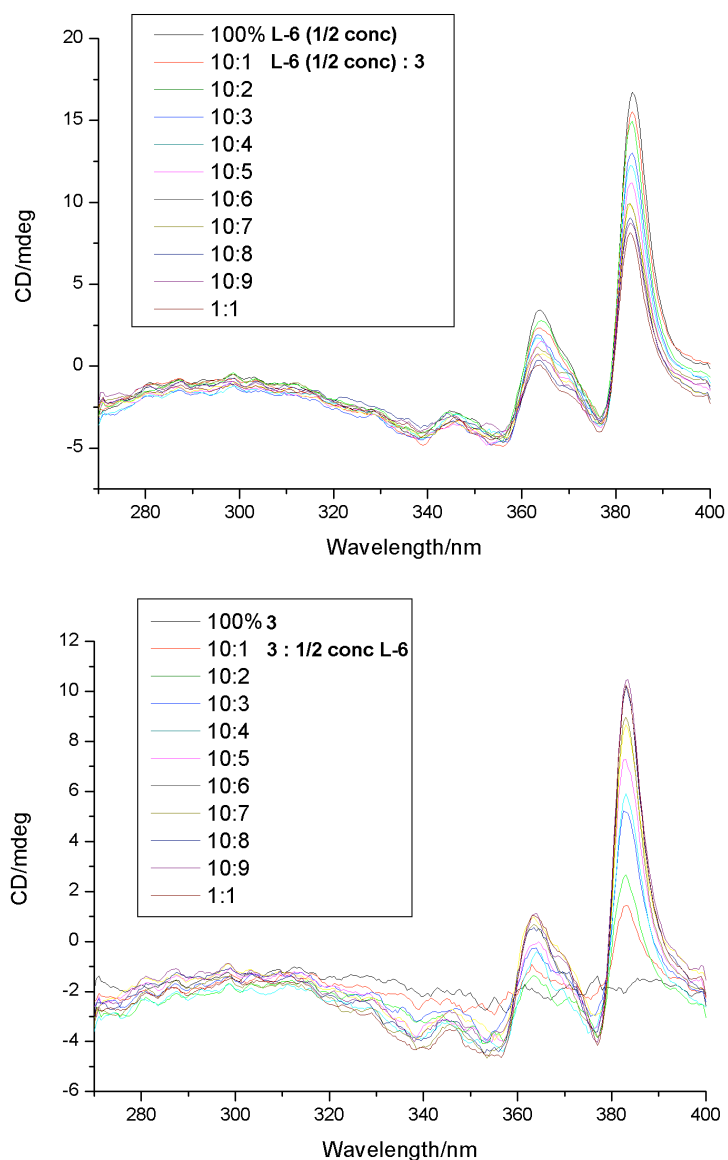


Figure S9. Raw experimental CD data for the second graph of **Figure 10** (black points). Concentration of **3** solution in TCE = $2.1 \times 10^{-4} \text{ mol dm}^{-3}$. Concentration of **L-6** solution in TCE = $1.05 \times 10^{-4} \text{ mol dm}^{-3}$.

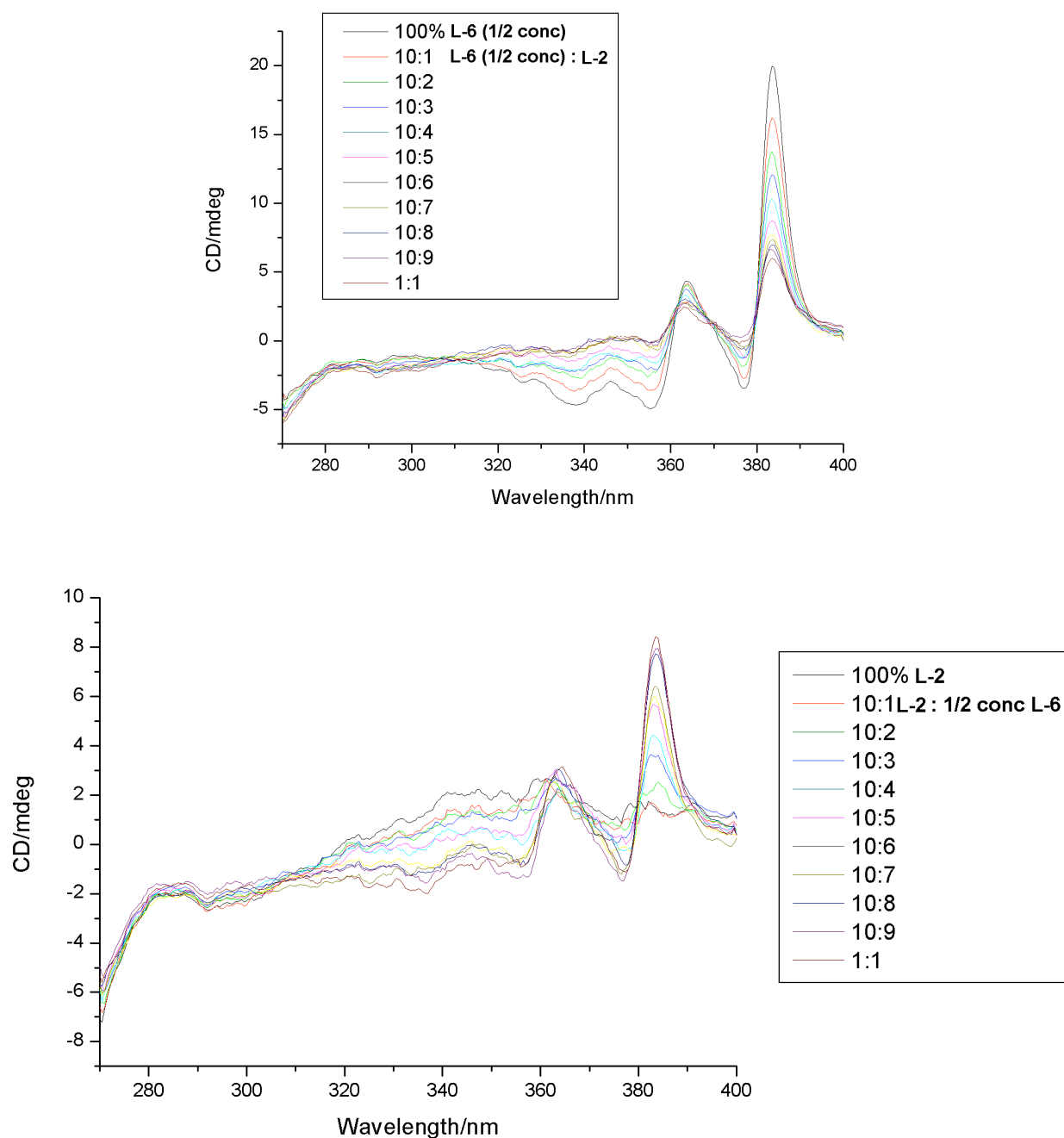


Figure S10. Raw control CD data for the second graph of **Figure 10** (red points). Concentration of **L-2** solution in TCE = 2.1×10^{-4} mol dm⁻³. Concentration of **L-6** solution in TCE = 1.05×10^{-4} mol dm⁻³.

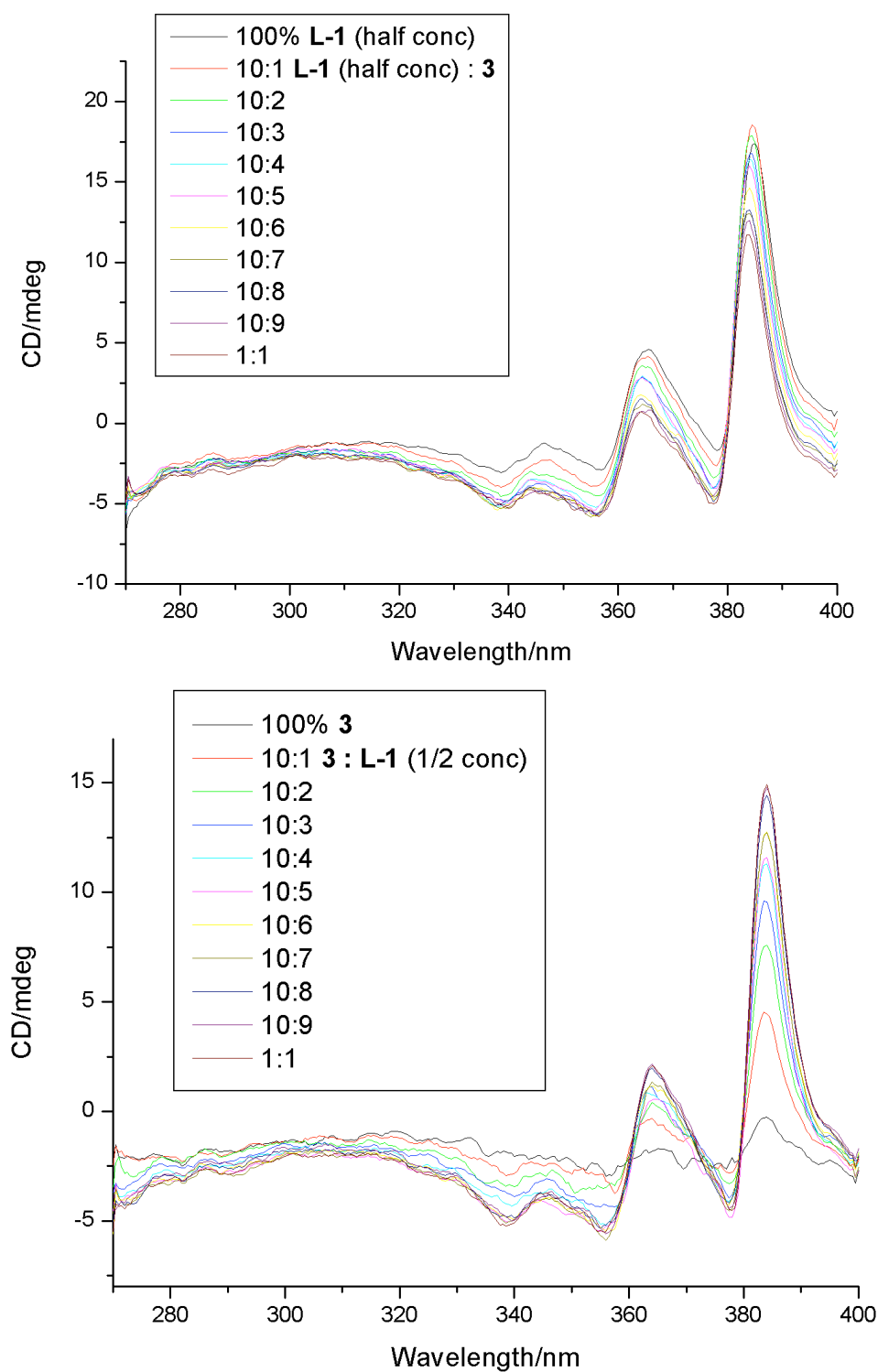


Figure S11. Raw experimental CD data for the second graph of **Figure 10** (blue points). Concentration of **3** solution in TCE = 2.1×10^{-4} mol dm⁻³. Concentration of **L-1** solution in TCE = 1.05×10^{-4} mol dm⁻³.

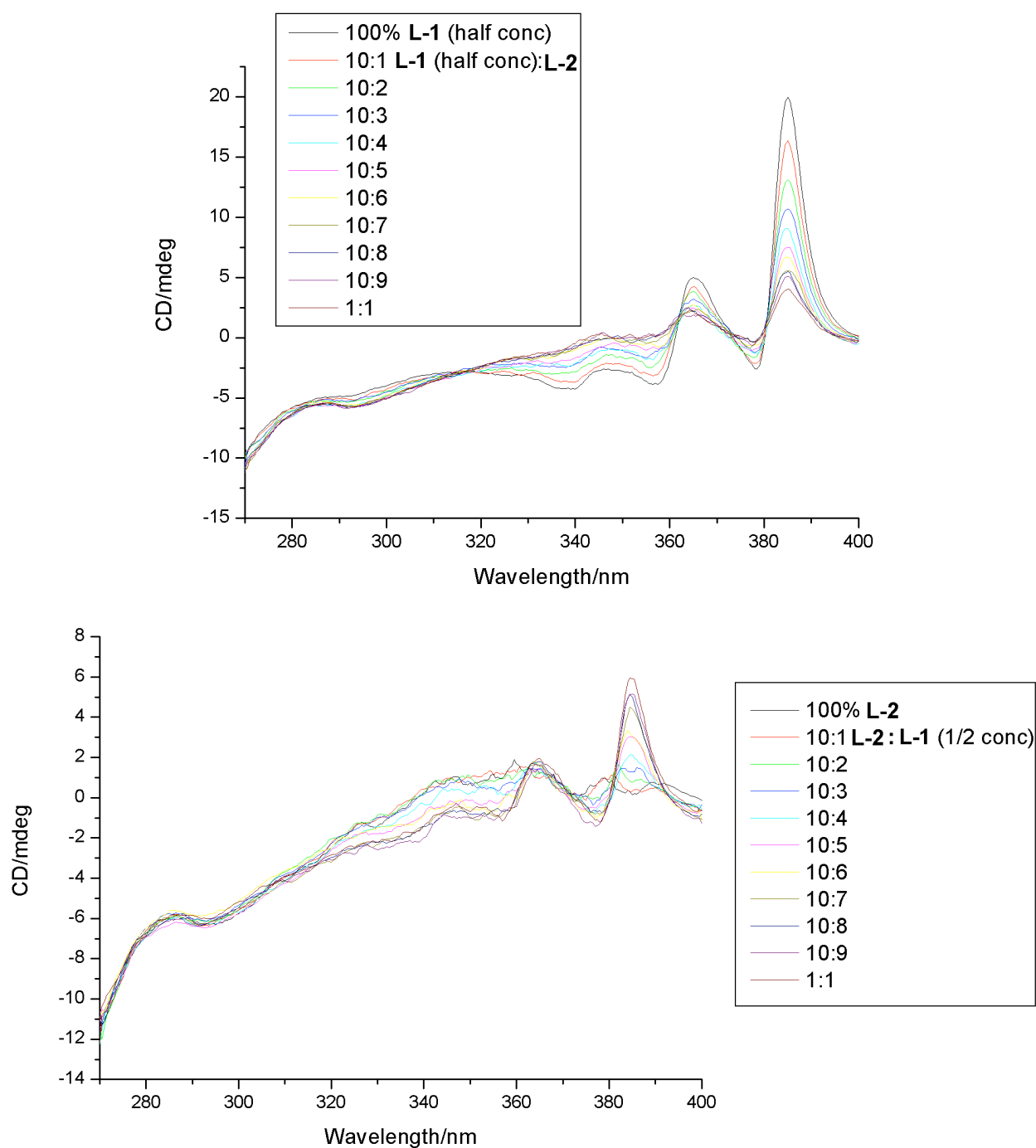


Figure S12. Raw control data for the second graph of **Figure 10** (orange points). Concentration of **L-2** solution in TCE = 2.1×10^{-4} mol dm⁻³. Concentration of **L-1** solution in TCE = 1.05×10^{-4} mol dm⁻³.

Figure 11 is made up of three sets of averaged experimental data. The raw data for these three runs, as well as the control dilution (see above) are given below.

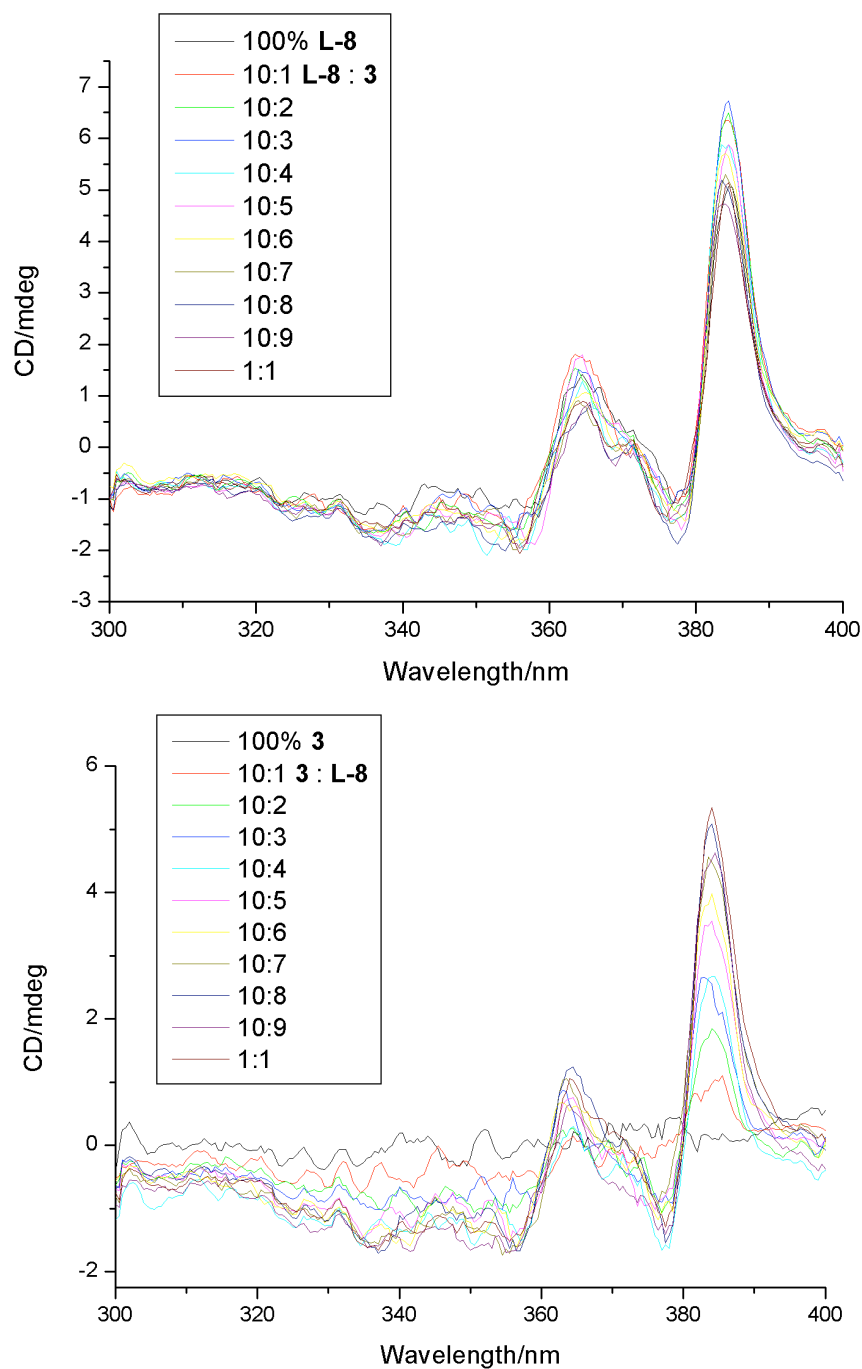


Figure S13. One of the three sets of raw experimental CD data averaged to make the data of which the black datapoints on **Figure 11** represent the CD_{max} . Concentration of both **3** and **L-8** solutions in TCE = 2.1×10^{-4} mol dm⁻³.

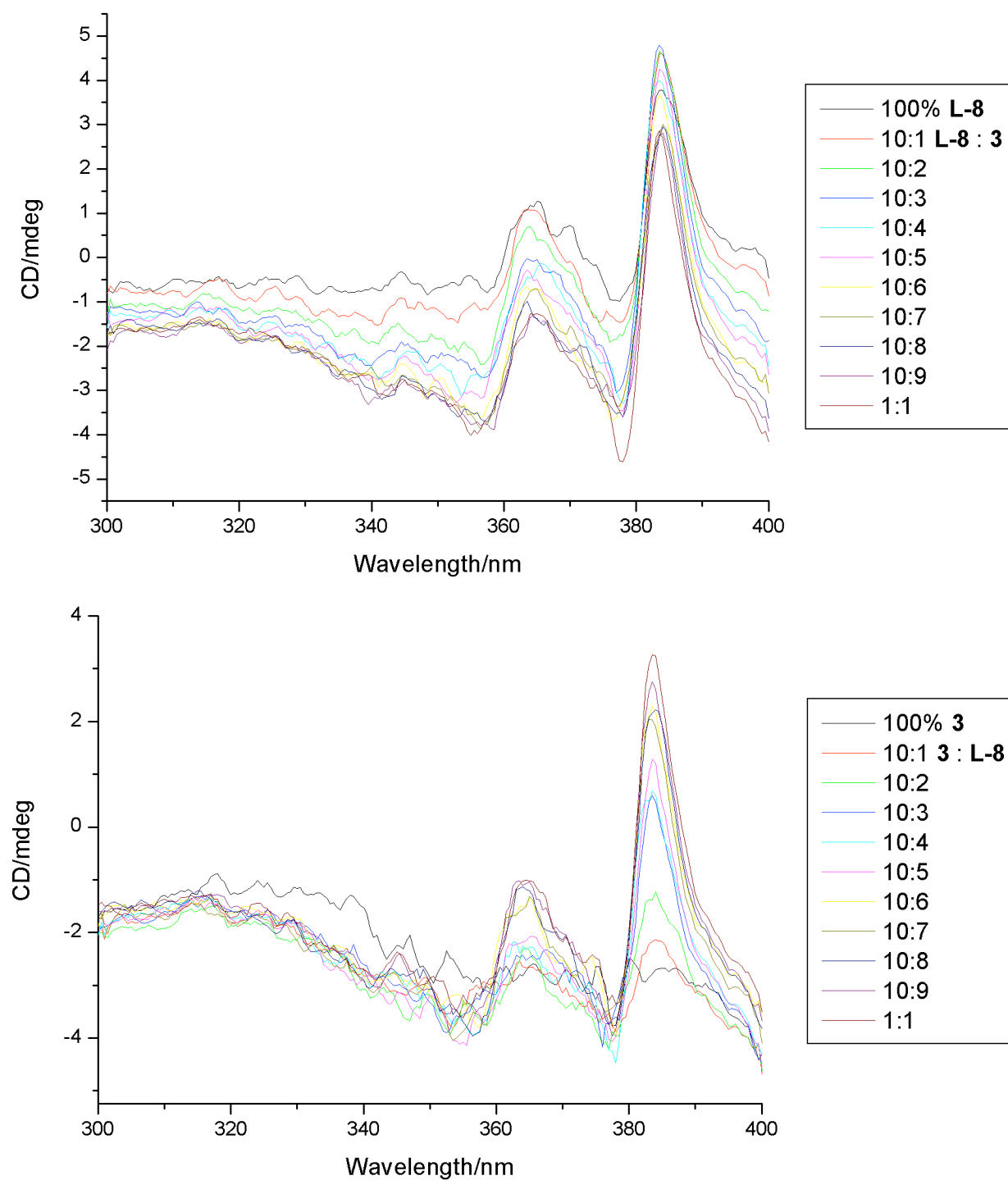


Figure S14. The second of the three sets of raw data averaged for **Figure 11**. Concentration of both **3** and **L-8** solutions in TCE = 2.1×10^{-4} mol dm⁻³.

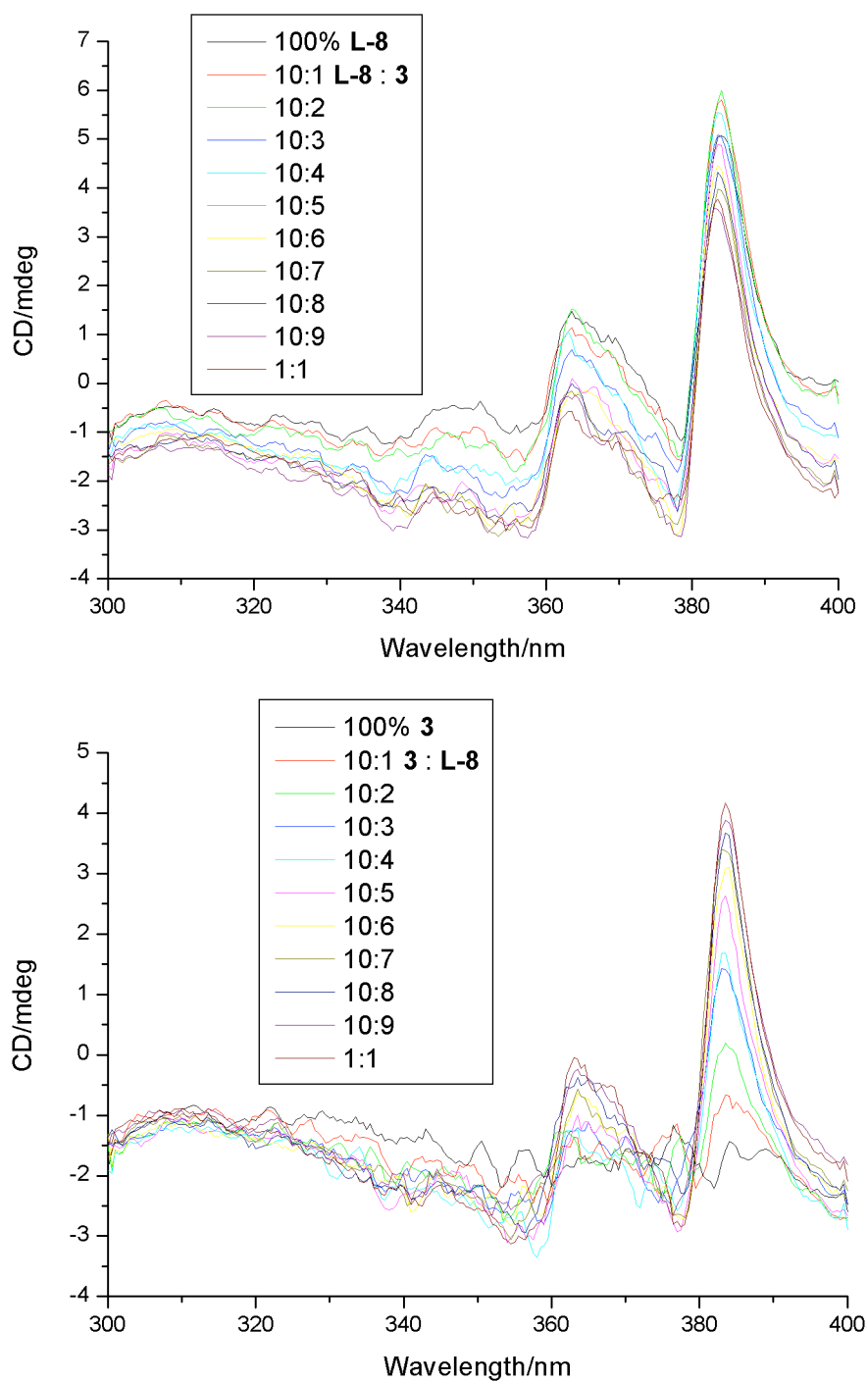


Figure S15. The third of the three sets of raw data averaged for **Figure 11**. Concentration of both **3** and **L-8** solutions in TCE = 2.1×10^{-4} mol dm⁻³.

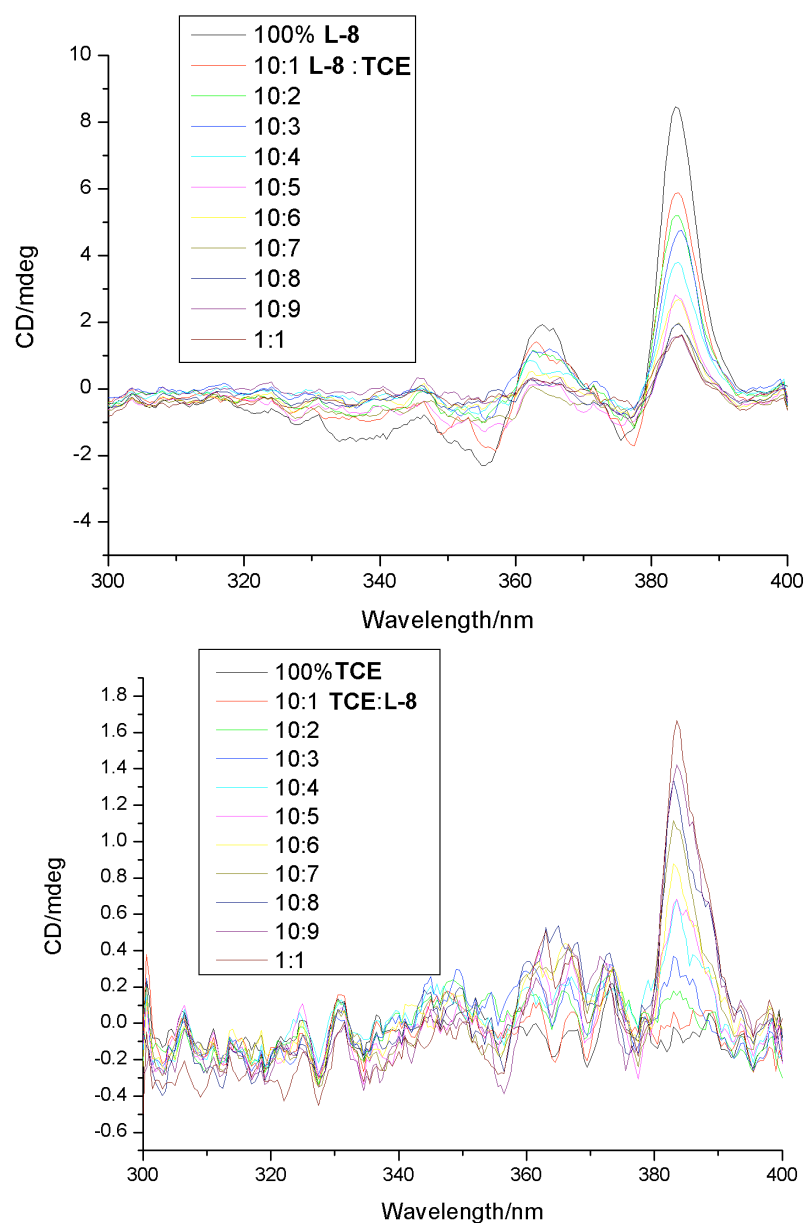


Figure S16. Raw data for the control dataset (red datapoints) on **Figure 11**. This used the dilution protocol described above. Starting concentration of **L-8** solution in TCE was $2.1 \times 10^{-4} \text{ mol dm}^{-3}$.

References

1. G. D. Pantos, P. Pengo and J. K. M. Sanders, *Angew. Chem.-Int. Ed.*, 2007, **46**, 194.
2. T. W. Anderson, J. K. M. Sanders and G. D. Pantos, *Org. Biomol. Chem.*, 2010, **8**, 4274.